Ocean heat budget analysis on sea surface temperature anomaly in western Indian Ocean during strong-weak Asian summer monsoon

Ibnu Fathrio[1,2], Atsuyoshi Manda[3], Satoshi Iizuka[4], Yasu-Masa Kodama[1], Sachinobu Ishida[1]
[1]Meteorological Laboratory, Graduate School of Science and Technology, Hirosaki University, Hirosaki, Aomori, Japan.
[2]National Institute of Aeronautics and Space of Indonesia, Bandung, West Java, Indonesia.
[3]Climate and Ecosystems Dynamics Division, Graduate School of Bioresources, Mie University, Tsu, Mie, Japan.
[4]Storm, Flood, and Landslide Division, National Research Institute for Earth Science and Disaster Resilience, Tsukuba, Ibaraki, Japan.

E-mail: ibnu.fathrio@lapan.go.id

Abstract. This study presents ocean heat budget analysis on seas surface temperature (SST) anomalies during strong-weak Asian summer monsoon (southwest monsoon). As discussed by previous studies, there was close relationship between variations of Asian summer monsoon and SST anomaly in western Indian Ocean. In this study we utilized ocean heat budget analysis to elucidate the dominant mechanism that is responsible for generating SST anomaly during weak-strong boreal summer monsoon. Our results showed ocean advection plays more important role to initate SST anomaly than the atmospheric prcess (surface heat flux). Scatterplot analysis showed that vertical advection initiated SST anomaly in western Arabian Sea and southwestern Indian Ocean, while zonal advection initiated SST anomaly in western equatorial Indian Ocean.

1. Introduction

Past studies revealed that there was close relationship between sea surface temperature (SST) in western Indian Ocean (WIO) and Asian summer monsoon (Southwest monsoon). Early numerical simulation found that colder SST anomalies in western Arabian Sea are responsible for reduced monsoon precipitation over Indian and adjoining areas [1]. This is accompanied with the increase in the moisture flux convergence and precipitation over south of the equator. Izumo et al. showed there is close relation between SST anomaly near Somali-Oman and precipitation in western Indian Continent [2]. They highlighted variations of ocean upwelling in boreal spring generates SST anomaly in Somali-Oman coast. Warming (cooling) of SST could increase (decreases) evaporation, which results in greater (less) moisture transport towards Indian continent. Izumo et al. argued that suppressed upwelling could be traced back to weak southwesterly monsoon wind generated by warm SST anomaly in the southwestern Indian Ocean [2].

Recent intensive ocean observation over Indian Ocean supported development of ocean reanalysis models by ocean data assimilation technique. It is expected that better understanding of ocean internal process over Indian Ocean can be achieved. Previous ocean

heat budget studies revealed that seasonal SST variation in WIO could be explained by variation of surface heat flux and oceanic process [3]. However, the role of internal ocean process to initiate boreal summer (June, July and August) SST anomalies in WIO was not fully discussed yet. Hence, this study aims to portray the ocean advection role to initiate strong-weak summer monsoon related SST anomaly by revisiting the ocean heat budget analysis over WIO.

2. Data and Method

In this study, four ocean reanalysis were used for analysis: GECCO2, SODA3, ORAS4 and GODAS. The time period of data was chosen from 1982 to 2012 (31 years) and we limit our area of analysis to WIO in 40-80E and 30S-30N. The SST was obtained from National Oceanic and Atmospheric Administration (NOAA) Optimum Interpolation (OI) version 2 (V2) data [4]. Surface winds data and surface radiation flux data that includes latent heat flux, shortwave radiation flux, longwave radiation flux, latent heat flux and sensible heat flux are obtained from National Centers for Environmental Prediction (NCEP)-National Center for Atmospheric Research (NCAR) [5]. These data were obtained from NCEP Reanalysis data provided by the NOAA/OAR/ESRL PSD, Boulder, Colorado, USA, from their Web site at https://www.esrl.noaa.gov/psd/.

We examined the SST anomaly over the WIO in ocean reanalysis models by analyzing the heat budget in the upper-50-m which is similar to [6-8] i.e.:

$$\frac{\partial T}{\partial t} = -u\frac{\partial T}{\partial x} - v\frac{\partial T}{\partial y} - w\frac{\partial T}{\partial z} + \frac{Q}{\rho_0 C_p H} + \mathrm{Re}\,sidual \qquad (1)$$

where T and u, v, and w represent the climatological monthly means of potential temperature (mixed layer temperature) and zonal, meridional, and vertical ocean current velocities, respectively, Q represents the surface heat flux into the ocean, H is a thickness of the water column, and C_p and ρ_0 denote the specific heat of seawater at constant pressure (set to 3994 J $kg^{-1}K^{-1}$) and a reference density of seawater (set to 1025 kg m^{-3}), respectively. All the terms were averaged over the upper 50 m in this study. The use of a fixed depth of 50 m avoids complications associated with an MME such as variations in the MLD amongst the models. In heat budget analysis, the ocean subsurface temperature over 50m is considered as mixed layer temperature (MLT). In chapter 3 we used MLT as proxy for SST. Because not all models provide surface heat flux data, we used surface radiation flux from NCEP-NCAR Reanalysis 1. All data were interpolated horizontally onto a 1° × 1° uniform horizontal grid, and interpolated vertically onto a 5-m uniform vertical grid (from the ocean surface down to 100 m) and a 25-m uniform vertical grid (below 100 m), using linear interpolation.

Monsoon index introduced by Kawamura was utilized to distinguish weak and strong monsoon during boreal summe [9]. This index was defined as meridional differences in area-averaged upper troposhpheric (200-500 hPa) thickness between Tibetian Plateau region (20-40N) and Northern Indian Ocean (0-20N and 50-100E) averaged in June, July and August (JJA) was calculated to determine the summer monsoon index. The positive (negative) index was considered as strong (weak) monsoon (figure 1). In this study, we only considered strong-weak years whose value greater than 0.5 of standard deviations. Kawamura [9] showed that this index correlate well with Webster and Yang's monsoon index [10].

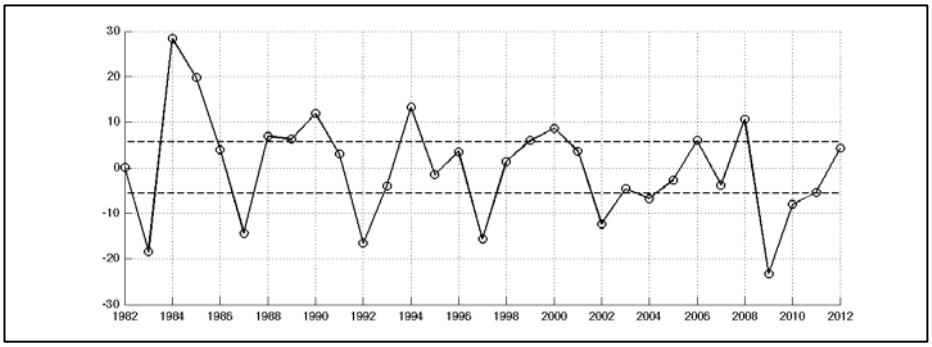

Figure 1. Time series of summer monsoon index for JJA defined by Kawamura (1998). The dashed line shows 0.5 of standard deviation value.

3. Results and Discussion

The differences between weak and strong composite of summer monsoon years in SST and surface wind are displayed in figure 2. The composite of weak monsoon years shows that warmer SST anomaly distributed over western Indian Ocean. This is accompanied by anomaly of surface northeasterly wind in the Arabian Seas and anomaly of northwesterly wind at the south of equator. Based on the SST anomaly distribution in WIO, we divided western Indian Ocean into three regions (shown by blue squares in figure 2) i.e. western equatorial Indian Ocean (WEIO, 45-60E and 10S-10N), western Arabian Sea (WAS, 50-65 °E and 13-23°N), and southwestern Indian Ocean (SWIO, 50-65°E and 5-15°S).

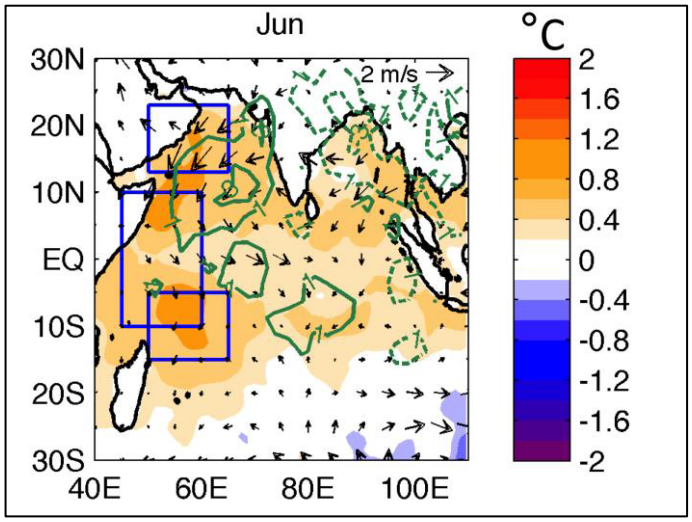

Figure 2. Composite of weak summer monsoon years minus composite of strong summer monsoon years for SST (°C, shaded), surface wind (m s^{-1}, vectors) and precipitation (mm day^{-1}, green contour with 2 mm day^{-1} interval) in February to July. Blue rectangles show region of study (see text for details)

3.1. Western equatorial Indian Ocean (WEIO)

In WEIO, MLT experiences annual variations with the warmest MLT presents in April-May (figure 3). The surface heat flux is the dominant cause of spring warming that peaks in March. In summer, cooling of MLT is caused by cooling of surface heat flux, vertical, zonal advection and residual term. Cooling in WEIO presents earlier than in WAS since the southwesterly monsoon wind was established first in WEIO. MLT recovers in autumn due to warming by meridional advection during June to August and surface heat flux in August to September. In contrast, vertical advection is against warming. It cools the MLT during boreal autumn.

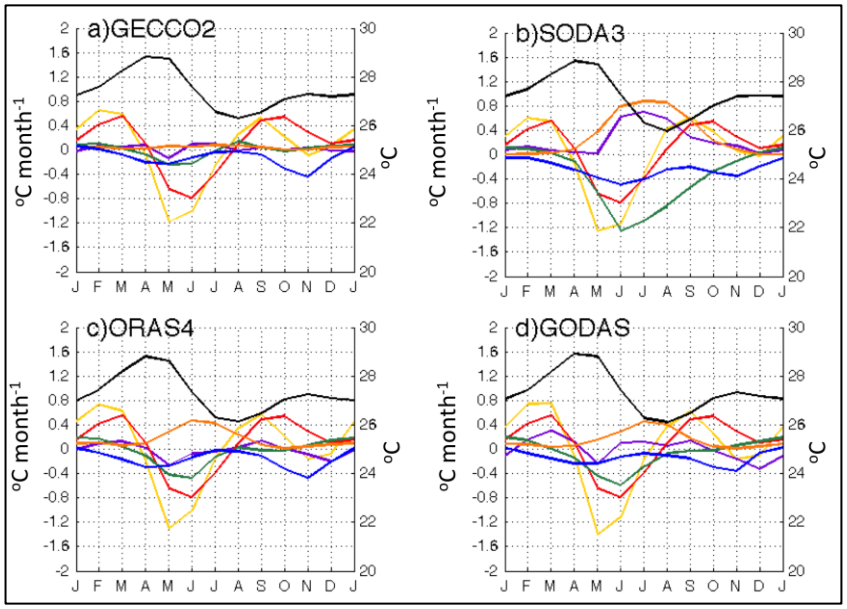

Figure 3. Area averaged monthly climatological time series of heat budget over western equatorial Indian Ocean for a) GECCO2, b) SODA3, c) ORAS4 and d) GODAS. Mixed layer temperature, mixed layer tendency, surface heat fluxes are denoted by black, yellow and red colors respectively. Vertical, zonal and meridional heat advections are denoted by blue, green and orange colors respectively. Residual term is denoted by purple color. The left y-axis is temperature tendency in °C month^{-1} and the right y-axis is mixed layer temperature in °C.

Differences between composite of weak and strong summer monsoon years are shown in figure 4. All models show that peak of positive MLT difference presents in June. This is preceded by positive MLT tendency difference in May. Scatterplot shows that MLT tendency in May and MLT monthly anomaly in June are well correlated (figure 5). It suggests that the ocean process in May could contribute to initiate the MLT monthly anomaly in June. We can clearly distinguish weak (blue dots) and strong (red dots) summer monsoon years. This implies that warm (cool) MLT anomalies in WEIO tend to occur during weak (strong) summer monsoon condition. In WEIO, the anomaly of MLT in June is well correlated with zonal advection (utm) process in May (figure 6 and table 1). This relation is shown as significant in all models. ORAS4 and GODAS showed that variation of vertical advection (wtm) and meridional advection (vtm) respectively could affect MLT monthly anomaly. Meanwhile, the zonal advection could be related to eastward transport of cold water from Omani and Somali upwelling regions [11-12]. Only GODAS that shows significant contribution of surface heat flux (hfx).

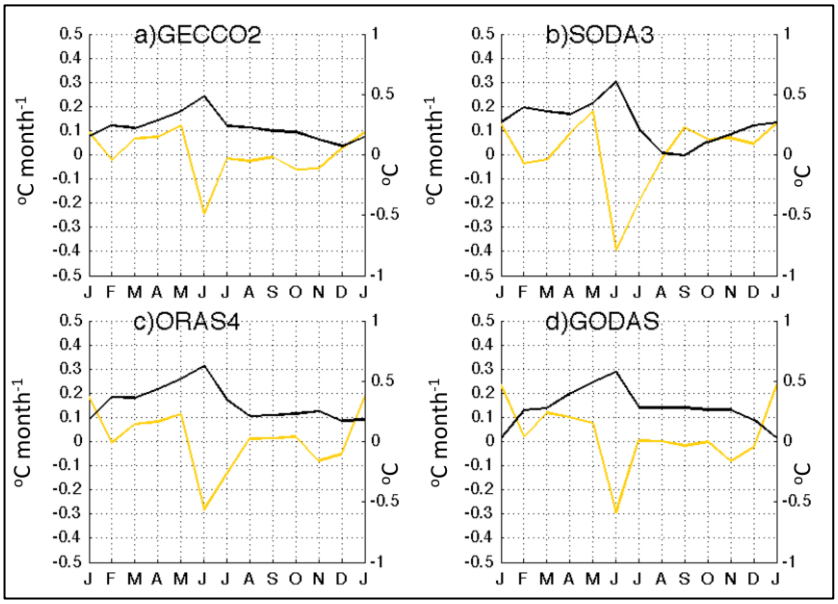

Figure 4. Time series differences for mixed layer temperature (black) and mixed layer temperature tendency (yellow) over western equatorial Indian Ocean for a) GECCO2, b) SODA3, c) ORAS4, d) GODAS. The left y-axis is temperature tendency anomaly in °C month^{-1} and the right y-axis is mixed layer temperature anomaly in °C.

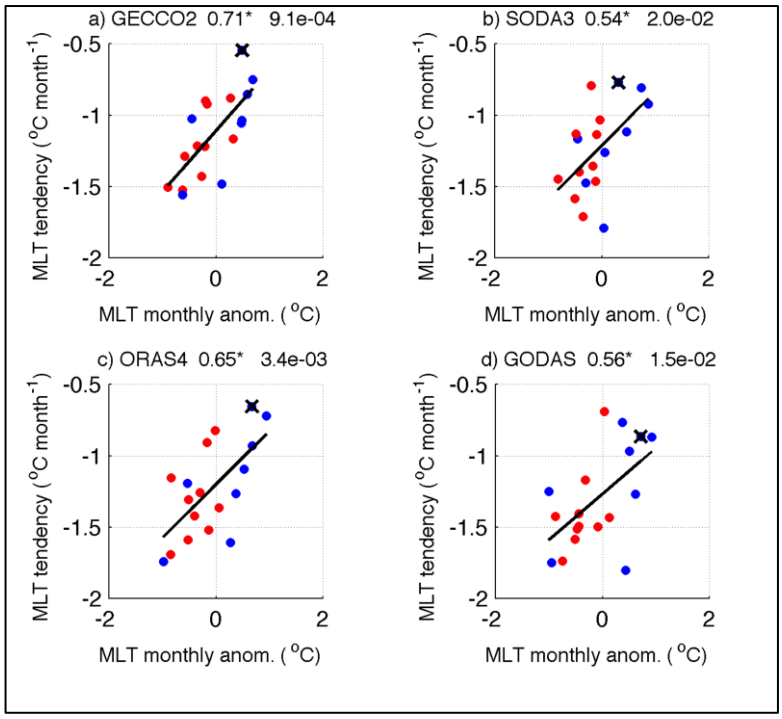

Figure 5. Scatterplot between MLT monthly anomaly in July and MLT tendency in June for western equatorial Indian Ocean. Blue and red dots indicate weak and strong summer monsoon years respectively. Cross (x) marker denotes year of 1997.

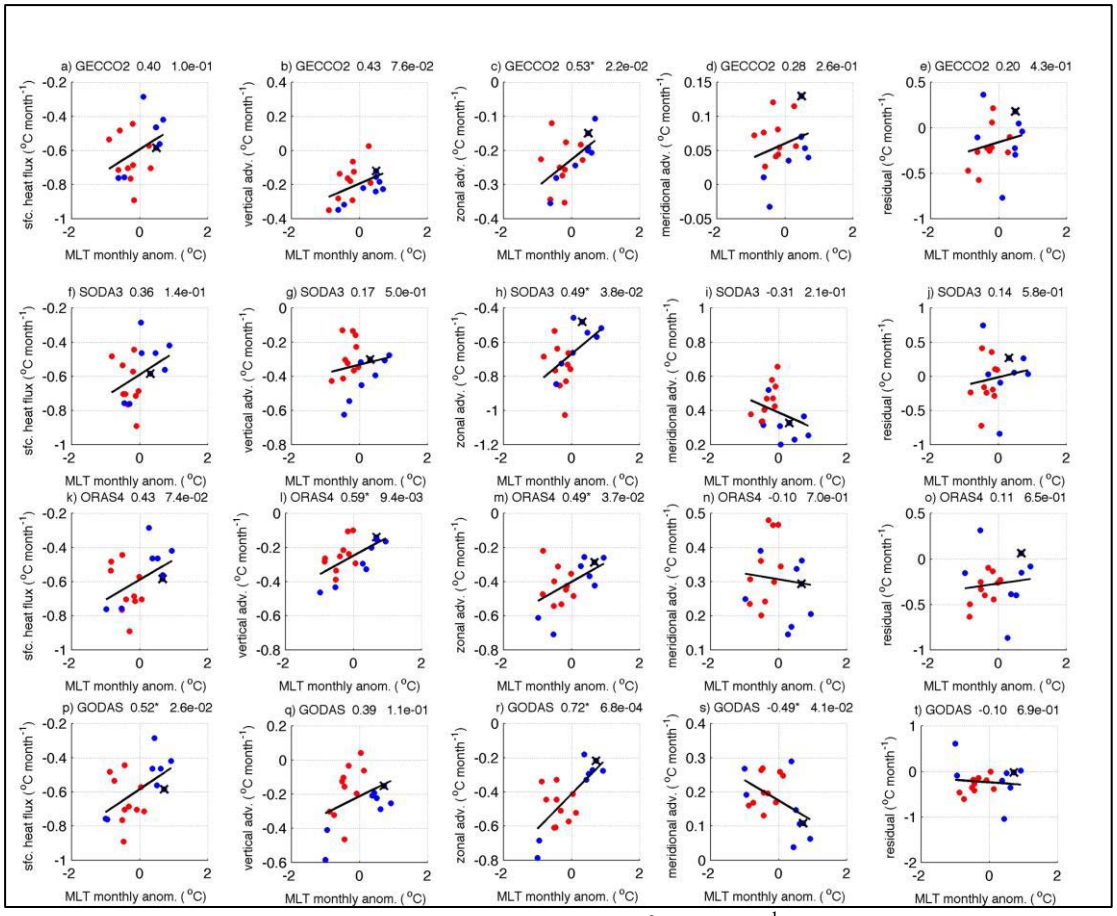

Figure 6. Scatter plot between heat budget terms (°C month^{-1}) in May and mixed layer temperature monthly anomaly (°C) in June for western equatorial Indian Ocean (45°-60°E, 10°S-10°N). The title in each panel, from left to right, indicate model's name, Pearson correlation coefficient and p-value respectively. Student t-test is used to determine p-value of correlations coefficient that is statistically significant at 5% level (P-value < 0.05) denoted by asterisk. Black solid lines indicate linear trend line. Cross (x) marker denotes year of 1997.

Table 1. Correlation between heat budget terms in May and mixed layer temperature anomaly in June for all models over western equatorial Indian Ocean. The abbreviation for dtm, hfx, utm, vtm, wtm and res stand for mixed layer tendency, surface heat flux, zonal advection, meridional advection, vertical advection, and residual term respectively. Correlation values that are significant at 95% level using student t-test are in blue color.

	GECCO2	SODA3	ORAS4	GODAS
dtm	**0.71**	**0.54**	**0.65**	**0.56**
hfx	0.40	0.36	0.43	**0.52**
utm	**0.53**	**0.49**	**0.49**	**0.72**
vtm	0.28	-0.31	-0.10	**-0.49**
wtm	0.43	0.17	**0.59**	0.39
res	0.2	0.14	0.11	-0.10

3.2 Western Arabian Sea (WAS)

In western Arabian Sea (WAS), MLT (black) experiences semiannual variations with two maximum in May-June and October-November (figure 7). The former maximum is warmer than the later one. The maximum temperature in May-June is preceded by warmest MLT tendency (yellow) in boreal spring (March-April). The main contributor for warming in boreal spring is the surface heat flux (red), which peaks in April. Penetrative of solar radiation is maximum due to clear-sky conditions and the thin mixed layer [11]. During boreal summer, the MLT tendency become negative accompanied by cooling of MLT.

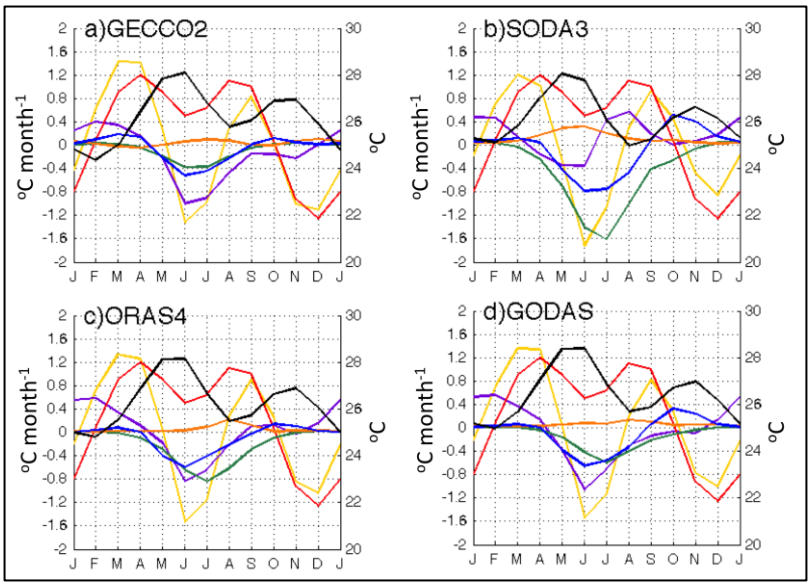

Figure 7. Similar to Figure 3 but for western Arabian Sea.

Warming of surface heat flux is suppressed in boreal summer, probably due to evaporation cooling. Summer cooling contribution also comes from vertical advection (blue) through wind-induced-upwelling, zonal advection (green) and residual term (purple) from May to September. In September-October, MLT start to warm again supported by warming of surface heat flux and suppressed cooling by vertical and meridional advection. After MLT reaches the second maxima in October-November, it slowly cools until reach the minimum point in January-February. This is probably caused by cooling of surface heat flux through evaporation induced by northeasterly monsoon wind.

Using similar approach applied in WEIO, time series difference between composite of weak and strong summer monsoon years were calculated. We found in all models that the largest positive MLT differences (black) present in July, preceded by largest positive MLT tendency differences (yellow) in May-June. To confirm this relation, scatter analysis was carried out. Figure 8 shows scatter plot between MLT in June and MLT tendency in May displays good correlation greater than 0.5 in all models. This robust relation explains that MLT monthly anomaly in July could be initiated by variation of heat budget components in May. Weak composite (blue dots) and strong composite (red dots) can be distinguished, except some outliers (blue dots) are caused due to unknown reason. This indicates that warm (cool) MLT anomalies in WAS tend to occur during weak (strong) summer monsoon years. Table 2 displays that MLT monthly anomaly is well correlated with vertical advection (wtm), surface heat flux (hfx) and zonal advection (utm). Highest correlation is shown by vertical advection in three models, except GECCO2. The second contributor is surface heat flux shown in three models, except SODA3. Zonal advection (utm) is another possible contributor process in GECCO2 and GODAS.

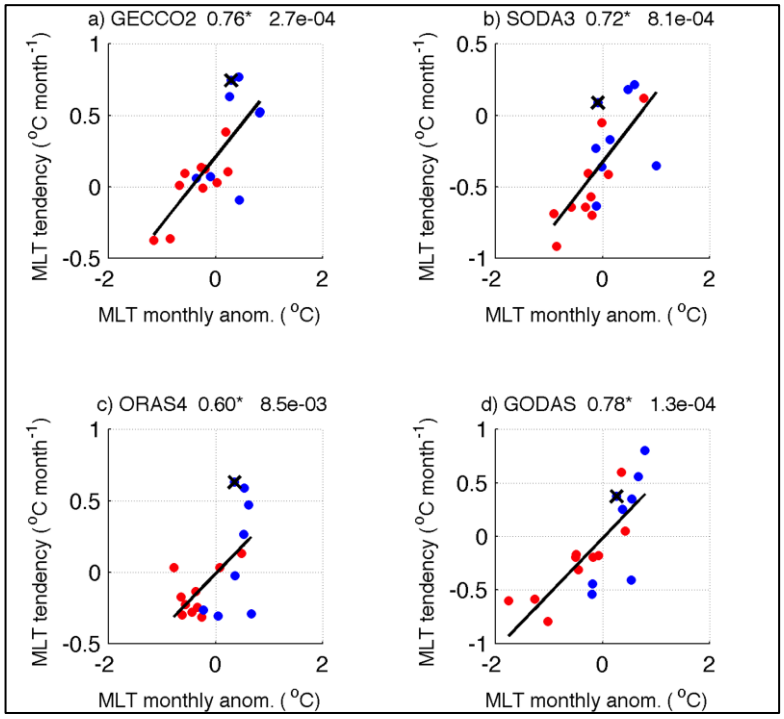

Figure 8. Scatterplot between MLT monthly anomaly in July and MLT tendency in May for western Arabian Sea. Cross (x) marker denotes year of 1997.

Table 2. Correlation between heat budget terms in May and Mixed layer temperature anomaly in July for all models over western Arabian Sea. The abbreviations and color are similar to Table 1.

	GECCO2	SODA3	ORAS4	GODAS
dtm	**0.76**	**0.72**	**0.60**	**0.78**
hfx	**0.54**	0.36	**0.58**	**0.55**
utm	**0.61**	0.24	0.27	**0.53**
vtm	0.11	0.34	0.13	0.16
wtm	0.11	**0.69**	**0.75**	**0.80**
res	0.16	0.15	0.04	0.43

3.3 Southwestern Indian Ocean

Mixed layer temperature displays annual variations that reaches maximum around March-April (figure 9). This is mainly attributed to warming by surface heat flux that occurs from October to March. In this season, radiation warming reaches maximum since the sun is located in the southern hemisphere. MLT reaches the coolest point during summer, preceded by cooling of surface heat flux contribution in boreal spring to summer. The vertical advection is against the surface heat flux. It tends to cool the MLT during boreal winter to spring. The meridional advection then contributes to warm the MLT in the late of summer. This owes to the southward Ekman heat transport associated strong meridional SST gradient and easterly wind stress associated with the Indian summer monsoon [13].

Similar approach (figure 4) was used by calculating time series difference in MLT and MLT tendency between weak and strong composite summer monsoon years in MLT and MLT tendency difference presents in March-April, preceded by positive MLT tendency difference in March. Figure 10 confirms that these two variables are well correlated. The MLT monthly anomaly in April could be initiated by atmospheric and/or oceanic process in March. Warm (cool) MLT anomalies also tend to present during weak (strong) summer

monsoon years. Table 3 displays correlation between MLT monthly anomaly in April and heat budget terms in March. Note that all models show significant contribution of vertical advection (wtm) in March to initiate MLT monthly anomaly in April, while the second contributor is surface heat flux (hfx). Our results are consistent with [13] which found that vertical advection process is responsible for warm MLT monthly anomaly on interannual time scale. Other possible contributor is residual term (res) that only shown in GECCO2 and SODA3.

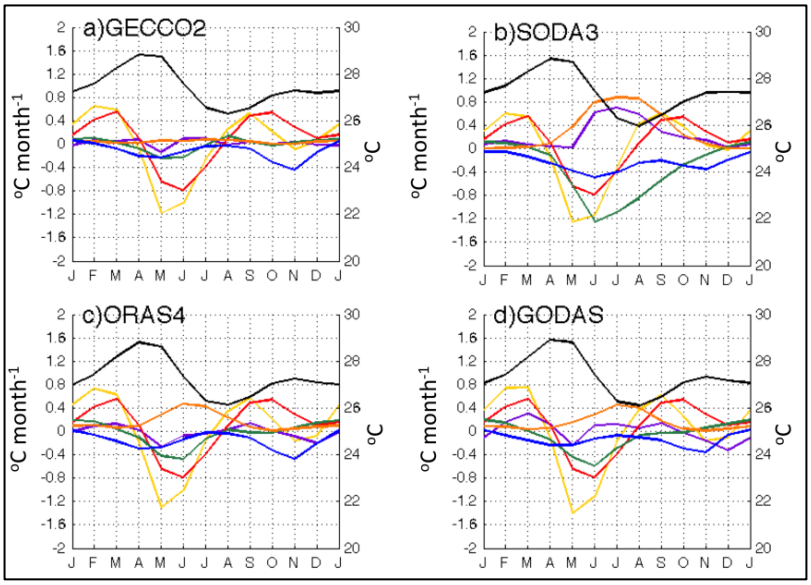

Figure 9. Similar to Figure 3, but for southwestern Indian Ocean.

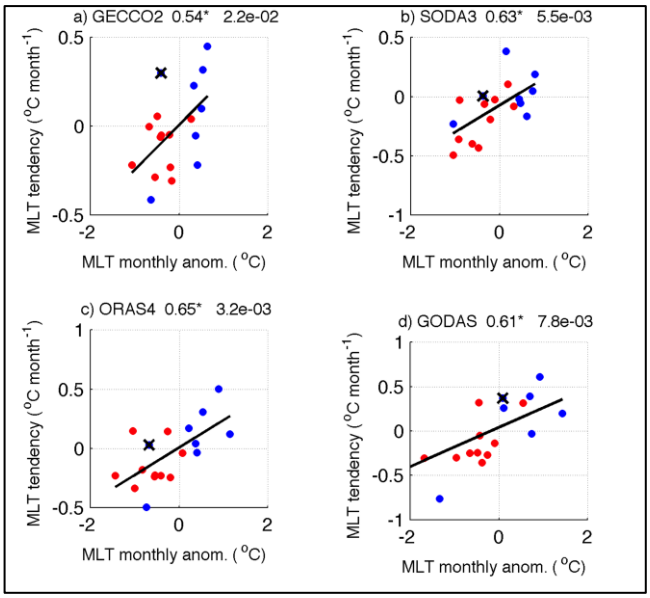

Figure 10. Scatterplot between MLT monthly anomaly in July and MLT tendency in May for southwestern Indian Ocean. Cross (x) marker denotes year of 1997.

During early development of El Nino 1997/1998 in March, it was recorded that Indian Ocean's SST also experience warming that exceed normal conditions in JJA 1997. This El Nino suppressed the monsoon circulation and induced convective activity in the east of Somalia coast [14]. Scatter analysis in Figure 5(WEIO), Figure 8(WAS) and Figure 10 (SWIO) clearly show that relatively warm MLT and MLT tendency in summer 1997 that

correspond to growing El Nino. Our results display (figure 6c, h, m and r) shows that during El Nino in 1997, cooling by zonal advection is more suppressed than in other years.

Table 3. Correlation between heat budget terms in March and mixed layer temperature anomaly in April for all models over southwestern Indian Ocean. The abbreviation is similar to Table 1.

	GECCO2	SODA3	ORAS4	GODAS
dtm	**0.54**	**0.63**	**0.65**	**0.61**
hfx	**0.59**	**0.67**	**0.54**	**0.57**
utm	0.37	0.13	**-0.54**	-0.31
vtm	-0.16	0.15	0.35	-0.02
wtm	**0.67**	**0.77**	**0.80**	**0.57**
res	**-0.48**	**-0.48**	-0.46	0.01

It is interesting to note that during boreal winter zonal advection becomes less important than the vertical advection in WEIO (table 4). Vertical advection (wtm) displays significant correlation in all models. It could be understood since during winter, climatologically, the thermocline is shallower than summer. As a result, the upwelling is easily affects the MLT/SST. During winter monsoon, the possible cause of thermocline variations is not only strong northeasterly wind. Indian Ocean Dipole (IOD) or El-Nino Southern Oscillation also could modulate the thermocline variation. The strongest impact may present when the IOD and ENSO co-occurred as in 1997 case. Figure 11 shows suppressed vertical advection in boreal autumn that is mainly contribute to warming compared to zonal advection which is associated with deepening of thermocline (isothermal of 20°C) up to 30m than in normal condition. Our results also corroborate [15] which emphasizes the importance of realistic ocean process to represent realistic SST in WIO. Insufficient cooling by ocean process may contribute to warm SST bias in WIO.

Table 4. Correlation between heat budget terms averaged in September, October, November and mixed layer temperature anomaly averaged in December, January and February for all models over western equatorial Indian Ocean. The abbreviation is similar to Table 1.

	GECCO2	SODA3	ORAS4	GODAS
dtm	**0.78**	**0.48**	**0.8**	**0.60**
hfx	**0.70**	0.16	-0.04	-0.10
utm	0.13	**0.48**	0.38	0.23
vtm	**0.70**	-0.25	**0.76**	0.35
wtm	**0.48**	**0.52**	**0.69**	**0.80**
res	-0.02	-0.43	-0.02	-0.13

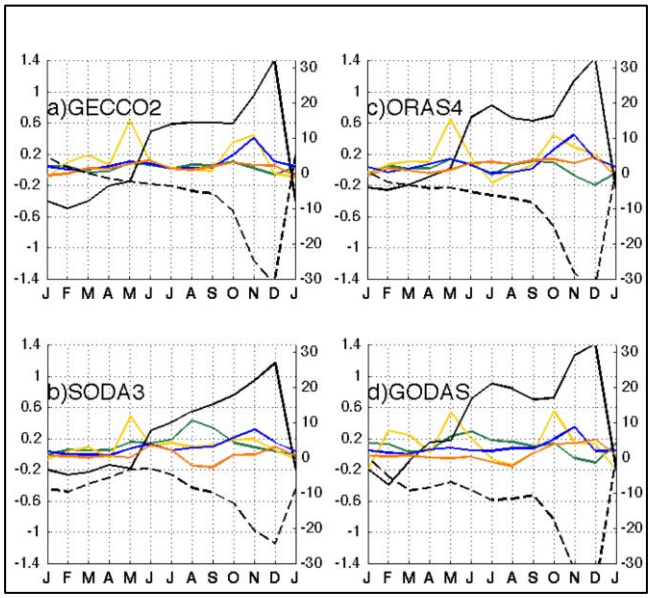

Figure 11. Time series difference of heat budget between El Nino 1997 case and monthly climatology. Black solid lines indicate difference in MLT (°C, right y-axis) and black dashed lines indicate thermocline (m, left y-axis). Solid lines in yellow color indicate difference in MLT tendency (°C month^{-1}, left y-axis). Solid lines in blue, green and orange colors indicate vertical advection, zonal advection and meridional advection respectively (°C month^{-1}, left y-axis).

4. Conclusion

Our result portrayed that ocean process plays more important role than atmospheric process (surface heat flux) to initiate the SST anomaly during extreme weak/strong summer monsoon conditions. Ocean heat budget analysis has been applied to analyze the SST anomaly during weak-strong southwest monsoon over on four ocean reanalysis models: GECCO2, SODA3, ORAS4 and GODAS. During weak summer monsoon, the SST anomalies tend to be warmer than usual, while during strong summer monsoon the SST anomalies tend to be colder than normal condition. During weak summer monsoon, at first the SST anomaly presents in SWIO intiated by vertical advection. Then the SST anomaly propagates northwards initiated by zonal advection in WEIO and vertical advection in WAS. The initiation process by ocean advection occurred about one-two month before MLT anomaly presents in WIO.

5. References

[1] Shukla J 1975 Effect of Arabian sea-surface temperature anomaly on Indian summer monsoon: A numerical experiment with the GFDL model *J. Atmos. Sci*. **32** pp 503–11

[2] Izumo T, Montegut C D, Luo J J, Behera S K, Masson S, and Yamagata T 2008 The role of the western Arabian Sea upwelling in the Indian monsoon rainfall variability, *J. Clim* **21** pp 5603–23

[3] Shaji C, Iizuka S, Matsuura T 2003 Seasonal Variability of Near-Surface Heat Budget of Selected Oceanic Areas in the North Tropical Indian Ocean *Journal of Oceanography* **59** pp 87

[4] Smith T M and Reynolds R W 2004 Improved extended reconstruction of SST (1854–1997) *J. Clim* **17** pp 2466–77

[5] Kalnay E The NCEP/NCAR 40-year reanalysis project 1996 *Bull. Amer. Meteor. Soc.* **77** pp 437-70

[6] Ng B, Cai W, Walsh K, Santoso A 2015 Nonlinear processes reinforce extreme Indian Ocean Dipole events *Sci. Rep*. **5** pp 11697

[7] Fathrio I , Manda A, IIzuka S, Kodama Y, Ishida S, 2017 Evaluation of CMIP5 models on sea surface salinity in the Indian Ocean *IOP Conf. Ser.: Earth Environ. Sci.* **54** 012039

[8] Fathrio I, Iizuka S, Manda A, Kodama Y, Ishida S, Moteki Q, Yamada H, Tachibana Y 2017 Assessment of western Indian Ocean SST bias of CMIP5 models *J. Geophys. Res. Oceans* **122** pp 3123–40

[9] Kawamura R 1998 A possible mechanism of the Asian summer monsoon-ENSO coupling *J. Meteor. Soc. Japan* **76** pp 1009-027
[10] Webster P J and Yang S 1992 Monsoon and ENSO: Selectively interactive systems *Quart. J. Roy. Meteor.Soc*. **118** pp 877-926
[11] Montégut C B, Vialard J, Shenoi S S, Shankar D, Durand F, Ethé C, and Madec G 2007 Simulated Seasonal and Interannual Variability of the Mixed Layer Heat Budget in the Northern Indian Ocean *J. Climate* **20** pp 3249–3268
[12] Shankar D, Vinayachndran P N, and Alallat U 2002 The monsoon currents in the northern Indian Ocean *Prog. Oceanogra*. **52 (1)** pp 63–120
[13] Yoko T, Tozuka T, and Yamagata T 2008 Seasonal Variation of the Seychelles Dome *J. Climate* **21** pp 3740–3754
[14] Shen X, and Kimoto M 1999 Influence of El Niño on the 1997 Indian summer monsoon *Journal of the Meteorological Society of Japan* Ser. II **77** (5) pp 1023-1037
[15] Yang W, Seager R, Cane M A, and Lyon B 2015 The rainfall annual cycle bias over East Africa in CMIP5 coupled climate models *J. Climate* **26** pp 9789–9802